

Respiratory Rate Estimation during Triage of Children in Hospitals

Syed Ahmar Shah, Susannah Fleming, Matthew Thompson, and Lionel Tarassenko

Syed Ahmar Shah is a Postdoctoral Research Assistant with the Institute of Biomedical Engineering, Department of Engineering Science, University of Oxford, Oxford, UK (e-mail: syed.shah@eng.ox.ac.uk).

Susannah Fleming is a Research Fellow with the Nuffield Department of Primary Care Health Sciences, University of Oxford, Oxford, UK (e-mail: susannah.fleming@phc.ox.ac.uk).

Matthew Thompson is a Professor with the Department of Family Medicine at University of Washington, Seattle, USA (e-mail: matthew.thompson@phc.ox.ac.uk).

Lionel Tarassenko is a Professor of Electrical Engineering and head of Department of Engineering Science, University of Oxford, Oxford, UK (e-mail: ; lionel.tarassenko@eng.ox.ac.uk).

Abstract— Accurate assessment of a child's health is critical for appropriate allocation of medical resources and timely delivery of healthcare in Emergency Departments. The accurate measurement of vital signs is a key step in the determination of the severity of illness, and respiratory rate is currently the most difficult vital sign to measure accurately. Several previous studies have attempted to extract respiratory rate from photoplethysmogram (PPG) recordings. However, the majority have been conducted in controlled settings using PPG recordings from healthy subjects. In many studies, manual selection of clean sections of PPG recordings was undertaken before assessing the accuracy of the signal processing algorithms developed. Such selection procedures are not appropriate in clinical settings.

A major limitation of AR modeling, previously applied to respiratory rate estimation, is an appropriate selection of model order. In this study, we developed a novel algorithm that automatically estimates respiratory rate from a median spectrum constructed applying multiple AR models to processed PPG segments acquired with pulse oximetry using a finger probe. Good-quality sections were identified using a dynamic template-matching technique to assess PPG signal quality. The algorithm was validated on 205 children presenting to the Emergency Department at the John Radcliffe Hospital, Oxford, UK, with reference respiratory rates up to 50 breaths per minute estimated by paediatric nurses. At the time of writing, we are not aware of any other study that has validated respiratory rate estimation using data collected from over 200 children in hospitals during routine triage.

Index Terms—Autoregressive (AR) models, respiratory rate, photoplethysmogram (PPG), pulse oximeters, pediatrics, vital signs.

I. Introduction

Accurate assessment of a child's health is critical for appropriate allocation of medical resources and timely delivery of healthcare in acute clinical settings such as Emergency Departments (EDs). Serious infections in particular, such as meningitis and pneumonia, account for 20% of deaths in childhood [42] and therefore require early recognition and treatment in order to minimize morbidity and mortality.

The accurate measurement of vital signs is a key step in the determination of overall severity of illness in triage (initial assessment) settings. Respiratory rate in particular is recognised as an important vital sign (usually estimated by nursing staff counting chest wall movements for 15 or 30 seconds) since it is predictive of lower respiratory infections or pneumonia [34, 39, 49], admission to hospital [4] and death [43]. However, it is measured by only 17% of general practitioners during their initial assessment of children (less than 5 years of age) [54]. This may be due to the inaccuracy of manual counting or to the lack of appropriate devices [23, 32, 52]. Current technology for directly measuring respiratory rate is not practical in many emergency or primary care settings, as it involves attaching electrodes to the chest or the use of nasal thermistors.

The photoplethysmogram (PPG) is routinely recorded during initial assessment of children in acute settings using a small finger or toe probe to measure heart rate and peripheral arterial oxygen saturation. Both the amplitude (Amplitude Modulation, AM) and the frequency (Frequency Modulation, FM) of the PPG signal have variations that reflect the respiratory rate [19, 36]. These modulations are caused by changes in peripheral blood volume directly or indirectly due to respiration. AM is primarily caused by the mechanical effects of respiratory-related movement in the thoracic region and diaphragm, while FM is caused by 'respiratory sinus arrhythmia' (heart rate increases during inspiration and decreases during expiration) [51]. Several previous studies have attempted to extract respiratory rate from PPG recordings [6, 9-11, 18-20, 26, 27, 29, 30, 33, 37, 56, 57]. However, the majority have been undertaken in controlled settings using PPG recordings from

healthy subjects [9, 11, 18-20, 26, 27, 29, 33, 37, 57]. In the few studies analyzing recordings from ill patients in clinical settings, manual selection of clean sections of PPG recordings was undertaken before assessment of the accuracy of the signal processing algorithms developed [6, 10, 30, 56]. Such selection procedures are not appropriate in real-world clinical settings.

Autoregressive modeling (AR) is a well-accepted method for estimating the power spectrum of a time series. Unlike the traditional periodogram, the frequency resolution does not depend on the number of data points. To increase the frequency resolution of the traditional periodogram, longer sequences are required. However, this is not feasible for physiological signals since stationarity cannot be assumed over longer periods. AR-based spectral estimation has been previously applied to a number of physiological signals, including the EEG [41], the intrapartum cardiotocogram [3] and the PPG [10].

AR modeling was first applied to the problem of extracting respiratory rate information from the PPG by Fleming and Tarassenko [10] using 14 five-minute clean sections of PPG recordings manually selected from the MIMIC database [14]. While the AR method was shown to outperform all existing methods at the time, a major limitation of the method is the susceptibility of model order choice to noise. Lee and Chon [26] reported an improved AR-based respiratory rate estimation which used the optimal parameter search (OPS) technique for AR-model parameter estimation. This method was compared with the widely-used Burg algorithm and model order selection based on the Akaike information criterion (AIC). The OPS method was superior to the Burg method over the whole range of respiratory rates studied. However, a major problem with this study [26] is that the model order selected for the Burg method (30) is too high. The PPG recordings were detrended, filtered and downsampled to 2 Hz, which meant that there were 15 poles in the range of 0 to 60 breaths/minute. With such a high number of poles, the assumption that only the pole lying at a certain angle, θ , determines the shape of the frequency spectrum at $\omega = \theta$ is no longer valid since there are other poles lying close by. Therefore, selecting the pole with the highest magnitude as the pole whose angle corresponds to the respiratory rate is not appropriate. This provides a plausible explanation for the comparatively poor performance of the Burg algorithm in [26].

In previous studies on estimation of respiratory rate from the PPG, motion artifact has been

identified as the major reason for poor performance of the processing algorithm. Moreover, there appeared to be significant deterioration in performance when algorithms were evaluated on data acquired from subjects in clinical settings without manual selection of high-quality PPG data. Due to the limited time available during triage of children in hospitals and the need for practical measurement devices, manual selection of good-quality signals is not an option. In addition, the use of any post-processing algorithm (e.g. particle filtering [27]) to counter the presence of artifacts due to motion is unlikely to be of value as the monitoring time (1-2 minutes) during initial assessment of most children in acute clinical settings is limited.

In this paper, we describe a modified AR-modeling based algorithm that, instead of selecting a pole with the highest magnitude, constructs a median spectrum from multiple sets of AR model coefficients and then selects the dominant frequency, in order to estimate respiratory rate. An algorithm based on dynamic template-matching to assess the PPG signal quality is also presented. The algorithm was validated on 205 children presenting to the Emergency Department at the John Radcliffe Hospital, Oxford, UK.

II. Methods

A. Pediatric ED Study Protocol

This study was carried out between January and August 2011 using data from 205 children presenting to the Emergency Department at the John Radcliffe Hospital, Oxford, UK. Reference respiratory rates were estimated by pediatric nurses (by counting chest wall movement for 15 or 30 seconds). The protocol for the study was approved by a local medical board ethics committee (South Birmingham Research Ethics Committee, UK). Temperature measurements and PPG recordings were acquired from children who presented to the Pediatric Emergency Department for an acute medical problem. The PPG waveform was recorded using a Bluetooth-enabled Nonin 4100 pulse oximeter and a tablet-PC (Toughbook CF-X, Panasonic) with analysis software developed in Visual Studio. The pulse oximeter measured heart rate, peripheral arterial oxygen saturation and peripheral perfusion and transmitted the data using a wireless Bluetooth radio link. The software running on the tablet PC also

allowed the nurse to enter the patient's date of birth, the temperature measured using a standard axillary temperature probe and the manual respiratory rate estimate (see **Figure 1**).

[Insert Figure 1]

The software automatically assigned a sequential identification number for each child. The same identification number was recorded on the consent forms that were subsequently used to seek consent from the parents for the use of the child's data for research purposes.

The typical duration of a PPG recording was 2 minutes, which was considered *a priori* as sufficiently long for deriving respiratory rate without affecting the clinical workflow. All the vital signs, along with the patient ID, date of birth, and the 16-bit PPG waveform data were stored in text files on the hard drive of the tablet PCs. The filenames included the patient's study ID, thereby ensuring that only data from consented patients was accessed.

B. PPG Pre-processing

The PPG waveform acquired from the pulse oximeter contains respiratory rate information in both its amplitude (AM) and frequency (FM) variations. Appropriate pre-processing (depending on AM or FM) is required to extract the "respiratory signal" whose periodicity then needs to be determined. In this work, we consider AM since respiratory rate estimation using FM requires the extraction of a time-series reflecting beat-to-beat changes in heart rate, typically using a peak detection algorithm. Peak detection algorithms require the appropriate selection of a threshold, a challenging task in the presence of dicrotic notches. In addition, even if an accurate time-series is obtained using peak detection, there will still be a need for interpolation in order to re-sample the unevenly sampled time-series evenly.

In order to extract the "respiratory signal" using AM, it is important to reduce the spectral components at the cardiac frequency as these would otherwise tend to dominate the spectrum and decrease the accuracy of placement of the pole associated with the respiratory frequency (the respiratory pole). A large number of previous studies have employed low-pass filtering in order to

eliminate the spectral components due to cardiac frequency. In this work, the PPG is, therefore, first de-trended and then filtered with a low-pass FIR filter using a Kaiser window, with a 5% ripple in the passband and 40dB attenuation in the stopband. The cutoff frequencies were decided according to the age of a child. For children up to 2 years of age, the transition band (from the edge of the passband to the edge of the stopband) was chosen to be 1.25 Hz (75 breaths per minute) to 2 Hz (120 breaths per minute) while for children over 2 years of age, a transition band of 0.7 Hz (42 breaths per minute) to 2 Hz (120 breaths per minute) was chosen. Application of the FIR low-pass filter with the chosen transition bands imposes a lower limit of 4 Hz for downsampling to avoid aliasing [44]. The PPG signal was in fact downsampled to 5 Hz, which ensured that all the poles model frequencies up to 2.5 Hz (corresponding to 150 breaths/minute). The original PPG waveforms were sampled at 75 Hz and the choice of a downsampling frequency of 5 Hz (i.e. 75/15) ensured that no interpolation was required for the downsampling step. The downsampling process enhances the ability to resolve spectral components (by allowing a given frequency range to be represented by a greater angle in the pole-zero plot) in the expected range of respiratory frequencies. **Figure 2** shows a raw 20-second PPG segment, and the corresponding processed waveform after detrending, low-pass filtering and downsampling to 5 Hz.

[Insert Figure 2]

C. AR Algorithm for Respiratory Rate Estimation

Background: Autoregressive modeling assumes that the current value of a time series can be predicted as a linearly weighted sum of the preceding p terms of the same series. The parameter p is the model order which is usually much smaller than the length of the sequence N ,

$$y(n) = \sum_{k=1}^p a_k y(n-k) + e(n) \quad (1)$$

where $y(n)$ is the current output of the time series ($t = n$), $y(n - k)$ is the time series output at $t = n - k$, a_k are the parameters of the system quantifying the linear relationship between the current output (i.e. at $t = n$) and the previous outputs at $t = (n - k)$, and $e(n)$ is the error term which is assumed to be normally distributed with zero mean and a variance of σ^2 .

The model order p determines the number of poles that are available to model the frequency spectrum of the PPG signal. For models with $p \geq 3$, there can be multiple poles with phase angles that lie in the expected range of respiratory frequencies.

The poles in the AR model occur in complex conjugate pairs and define the spectral peaks in the power spectrum. The magnitude (m_k) and the angle of the k^{th} pole (θ_k) determine the magnitude of the spectral peak and the frequency at which it occurs [40]. The nearer the pole is to the unit circle on the pole-zero plot in the z-domain, the higher is the corresponding peak in the frequency domain [40]. The frequency f associated with a given pole is related to the phase angle θ of that pole according to $\theta = 2\pi f \Delta t$, where Δt is the sampling interval of the original sequence.

Previous work [9, 26, 27] has attempted to identify the pole with the highest magnitude as the pole corresponding to the respiratory rate. This, however, assumes that the different poles in the complex plane are far away from each other and therefore that the contribution of the k^{th} pole to the magnitude of the frequency spectrum is only at the frequency corresponding to θ_k . However, this assumption becomes much less valid when there are a large number of poles in the complex plane, 11 in [9] and 30 in [26] as illustrated in

Figure 3. Although the spectra shown in Figure 3(c) are similar, with the corresponding peaks lying close to each other, choosing the pole with the highest magnitude can lead, for a given model order, to erroneous estimation of the dominant frequency (the respiratory frequency). This is because a dominant peak can be either modelled by a single pole with a large magnitude (see

Figure 3(a)) or several poles with smaller magnitudes lying close to each other (

Figure 3(b)). Consequently, choosing a pole based on magnitude when the model order is large can lead to erroneous results. To address this problem, instead of finding the pole with the highest magnitude as was done previously [9, 26], we find the corresponding frequency spectrum from the poles identified. In order to do this, an n^{th} order AR model is applied to the processed PPG time-series (the “respiratory signal”) to obtain n poles. This is done by applying the z-transform to equation (1) to obtain the following equation:

$$\frac{Y(z)}{E(z)} = H(e^{j\omega T}) = \frac{1}{1 - \sum_{k=1}^n (1 - a_k)} \quad (2)$$

and then evaluating $|H(e^{j\omega T})|$ in the upper half of the unit circle ($\omega=0$ to π). The peak in the frequency spectrum is then identified and taken to correspond to the respiratory frequency (the estimated respiratory rate). This approach will be referred to as $AR_{spectrum}$ and the original approach of identifying a pole with the highest magnitude will be referred to as $AR_{original}$ henceforth (illustrated in Figure 4).

[Insert Figure 3]

As mentioned previously, another major challenge in using AR modeling is the appropriate selection of a model order. A number of approaches were considered for finding an optimal model order including Akaike’s Information Criterion [21], final prediction error [21], minimum description length [35], and observing the residual error as the model order was increased. In the novel method proposed in this work, rather than finding a single optimal model order, a set of autoregressive models of different model orders ($p = 2$ to 20) are considered. For each p , a corresponding $|H_p(e^{j\omega T})|$ is evaluated at M (1024) equally spaced points on the upper unit circle ($\omega=0$ to π). This corresponds to a frequency range of 0 to $f_s/2$ where f_s (the downsampled frequency of the processed

PPG) was chosen to be 5 Hz. Finally, a median spectrum $|H_{median}(e^{j\omega T})|$ is constructed by evaluating a median at each of the 1024 points. This method will be referred to as $AR_{medianspectrum}$ henceforth. **Figure 5** illustrates the construction of a median spectrum from various spectra and also shows the reference and the estimated respiratory rate.

[Insert Figure 4]

[Insert Figure 5]

In order to compare $AR_{medianspectrum}$ with $AR_{spectrum}$ and $AR_{original}$, a model order of 7 was chosen for $AR_{spectrum}$ and $AR_{original}$ as this was found to be the optimal choice using the Burg algorithm for parameter estimation on a subset of the available PPG data, similar to the approach adopted in [10].

D. Deterioration of PPG signal quality due to motion artifact

Corruption of the PPG signal as a result of motion artifact is a phenomenon recognised in several previous studies [28, 38, 48]. Motion artifact is a barrier to the efficient and reliable use of the PPG for extracting vital sign information. For illustration, **Figure 6** shows the PPG recording from a patient and the corresponding respiratory rate estimated using a 60-second sliding window with the corresponding estimate plotted at the centre of the window. In the figure, the estimate at $t=30$ is much lower than the reference respiratory rate (shown in green) as a result of a corrupted PPG segment between $t=20$ and $t=40$. As the sliding window moves forward and the PPG segment is no longer affected by motion artifact, the difference between the estimated respiratory rate and the reference decreases. The estimates at $t=130$ and $t=140$ are also erroneous, as the PPG segment is again corrupted by motion artifact.

[Insert Figure 6]

Previous techniques dealing with motion artifact in the PPG can be divided into two main types: (i) techniques that suppress the motion artifact, (ii) techniques that identify good-quality segments of PPG and subsequently process only those segments.

A number of approaches rely on finding a reference signal to provide an input to an adaptive filtering scheme and suppress the artifact introduced in the PPG as a result of motion (typically referred to as ‘noise’). These include the use of accelerometers [1, 12, 47] or an additional optoelectronic sensor [5] to quantify the noise. There have also been attempts to find the reference signal without the need for any extra hardware. This includes identifying the uncorrupted sections of a PPG signal and then using it to estimate a synthetic reference signal [7]. Finding a reference signal without any extra hardware is also the methodology implemented by the Masimo Corporation in their motion-resistant pulse oximeters. Their approach assumes that venous blood is a major contributor to the noise during motion. A venous noise reference is then extracted and used to suppress artifacts using adaptive noise cancellation [15]. Another technique to suppress motion artifact is the use of a filter bank and a matched filter [28]. The techniques adopted in [15, 28] use both the red and infrared channels to estimate the reference signal. Other techniques include modeling the motion artifact and taking the inverse of the model to eliminate the noise [16], using wavelet transforms [25], singular value decomposition [45, 46], Fourier series analysis [45] and independent component analysis [22].

The alternative approach which we adopt for dealing with motion artifact is to detect segments of PPG waveform that are contaminated by artifact, so that we consider only good-quality segments for further analysis. Signal-quality analysis includes the use of higher-order statistics [24], morphological analysis [8, 53] and template matching [55]. Extracting respiratory rate information from only good-quality signals will improve the accuracy of the estimate and also increase the confidence in the estimate.

Krishnan et al. [24] used skew and kurtosis measures and the detection of quadratic phase coupling using bispectral analysis to differentiate between clean and corrupted PPG segments. However, their

study included data from only 2 subjects and a window of fixed duration was used in the analysis. The work by Deshmane et al. [8] and Gil et al. [13] used Hjorth parameters to determine thresholds for making decisions on signal quality. The Hjorth parameters characterize the morphology of a signal by its activity, mobility and complexity [17]. Gil et al. [13] recorded PPG data from 9 pediatric patients and used a fixed window length of 5 seconds to compute Hjorth parameters and associated thresholds. The problem with using a fixed window length is that patients with different heart rates will have a different number of beats lying within a window. This will lead to a large spread of these morphological parameters making it challenging to find an optimal threshold. Deshmane et al. [8] partly addressed this problem by finding thresholds on adult patients under four different conditions, namely patients with asystole, extreme bradycardia, extreme tachycardia and ventricular tachycardia using 2-second non-overlapping windows. We could not investigate the use of Hjorth parameters on our 205-patient database, because the heart rate variation is very high (from 53 to 197 beats per minute). Fixed window length based approaches will therefore lead to poor signal quality estimation for the PPG signal recorded from children.

One solution to circumvent the problem caused by variation in heart rate is to assess the PPG signal beat-by-beat. This is the approach adopted in our study.

E. Algorithm for deriving SQI (Signal Quality Index)

Our algorithm for deriving a signal quality index combines beat-by-beat analysis with template matching [31] as illustrated in **Figure 7**. Firstly, beat onsets are determined for the PPG signal acquired from a patient using the beat onset algorithm described in [50]. A template is then created for the PPG recording by taking the mean of all the beat-to-beat segments in the first 30-second window. Every beat-to-beat segment in those first 30 seconds is compared to the template created by computing a correlation coefficient, and a threshold (chosen empirically) is applied to decide if the corresponding segment is of good or poor quality. A new template is then created from the good-quality segments. Subsequently, every beat-to-beat segment in the first 30 seconds (0-30 second data) is again compared to the internally validated template to decide if the corresponding beat segment is of good or poor quality. Once a decision has been made for the beats in the first 30-second window,

the beat-to-beat segments of the next 30-second window (30-60 second window) are then compared with the template to identify good-quality beats. The template is again updated using the good-quality beats identified in these 30 seconds (30-60 second window). This updated template is then used to identify the good-quality beats in the next 30 seconds of the signal (60-90 second window) followed by template update (see **Figure 7**). The cycle is repeated until the whole PPG recording for a patient has been analyzed.

[Insert Figure 7]

Figure 8 shows a 30-second PPG segment and the signal quality index with a value of +1 for a good-quality beat and a value of -1 for a poor-quality beat.

[Insert Figure 8]

III. Results

In this work, a 60-second sliding window (with an overlap of 50 seconds) was used and the mean of respiratory rates from each of the windows over the short monitoring period taken as the estimated respiratory rate. A greater overlap (50-seconds) between consecutive windows ensures that any estimation in error due to short corrupt segments can be filtered out during the post-processing stage.

Table I reports the mean and median absolute error and the number of patients for whom the estimated respiratory rate is within 5 breaths per minute of the reference respiratory rate. It can be seen that constructing a spectrum from an AR model ($AR_{spectrum}$), instead of selecting the respiratory pole based on magnitude only ($AR_{original}$), improves the performance of respiratory rate estimation. There is further improvement once multiple AR models with different model orders are computed and the median spectrum used for respiratory rate estimation $AR_{medianspectrum}$.

[Insert Table I]

The pediatric Emergency Department study included a qualitative assessment by the nurses of patient compliance using a 4-point scale developed for the study (compliant, intermittent movement, frequent movement, or non-compliant). In the current context, the term compliance refers to both voluntary and involuntary movements (e.g. coughing, yawning, crying etc.). The mean percentage of good-quality signal, using the SQI described above, was significantly lower in children assessed as “non-compliant”, or with “frequent movement” (46% vs 81%, $p < 0.0001$). **Table II** shows the performance of the algorithms with varying signal quality and as expected, the respiratory rate estimation algorithm improves as the signal quality improves.

[Insert Table II]

Table III reports the mean and median absolute error of the three methods in two age groups. It can be seen that the biggest improvement in performance after employing the $AR_{medianspectrum}$ occurs in the older age group (5-12y).

[Insert Table III]

Lastly, **Figure 9** shows the Bland-Altman plot [2] comparing the respiratory rates with scatter plot which compares the respiratory rate estimated from the “ $AR_{medianspectrum}$ ” algorithm with the reference respiratory rate estimated by the nurses, of all PPG recordings with an SQI of at least 80% ($n=126$). The mean difference between the two measures is 0.9 breaths per minute with a standard deviation of 8.6 breaths per minute. It is worth pointing out that the normal respiratory rate of children varies much more than adults (12 to 50 breaths per minute in this study).

[Insert Figure 9]

IV. Discussion

Unlike previous studies that estimated respiratory rate in experimental settings, or modified the clinical workflow, the strength of this study is that it was undertaken by pediatric nurses with no modification to their existing clinical workflow and without the introduction of any additional hardware to be attached to the patient.

One limitation of our study is the inaccuracy of the reference respiratory rate, as it was not considered feasible to attach additional sensors to collect a more reliable reference respiratory rate. However, Simoes et al. [52] compared the respiratory rate estimated by manual counting with that obtained using electrical impedance pneumography, with chest electrodes. They found that the standard deviation of the difference between respiratory rates estimated using manual counting and that obtained using chest electrodes was 8.6 breaths per minute, with a mean difference of 1.72 breaths per minute. As mentioned earlier, after repeating this calculation for our data, we obtained the same value for standard deviation with a slightly lower mean value. This suggests that the variance of the difference between respiratory rate estimated by manual counting and using electrical impedance measurements using chest electrodes is comparable to the difference between respiratory rates obtained by manual counting and that obtained with our algorithm for processing the PPG waveform.

Moreover, the impedance electrical impedance pneumogram recordings in [10] were displayed on a strip chart (and respiratory rate estimated from measuring the interval between peaks); any signal corruption due to movement artifact was manually removed. It is thus likely that the inaccuracy of respiratory rate estimation in the Simoes et al. study was primarily caused by human error, for example whenever the child was crying, coughing, yawning, agitated or being fed. This was further corroborated by the investigation of the counting failures which found that respiratory disease did not increase the number of counting failures [52]. On the other hand, 19% of all counting failures were due to agitation and 9% of all counting failures were due to the observer getting distracted and/or losing track of time.

V. Conclusion

Our work presents an algorithm for respiratory rate estimation, which use PPG acquired from a portable, non-invasive pulse oximeter probe. The algorithm was validated on 205 children with a wide range of respiratory rates, from 14 to 50 breaths per minute. These children were assessed during routine clinical practice in an Emergency Department. The errors obtained were similar to that

previously reported using ECG electrodes and electrical impedance pneumography [52]. This study thus provides a feasible option to estimate respiratory rates of children during assessment in Emergency Departments, especially if segments of PPG data corrupted by movement artifact are automatically discarded by an appropriate algorithm, such as the one presented in this paper

Acknowledgements

The author would like to acknowledge the Research Nurses in the Emergency Department at the John Radcliffe Hospital, Oxford (Sally Beer, Karen Warnes and Soubera Yousefi), who were funded by the NIHR Biomedical Research Centre, Oxford.

Declaration of interest

This paper presents independent research commissioned by the National Institute for Health Research (NIHR) under its Programme Grants for Applied Research funding scheme (RP-PG-0407-10347). The views expressed in this paper are those of the author(s) and not necessarily those of the NHS, the NIHR or the Department of Health. Informed consent was obtained from the parents of children whose data was used in this work. We have no conflicts of interest to declare.

REFERENCES

1. Asada, H.H., H.-H. Jiang, and P. Gibbs. (2004) *Active noise cancellation using MEMS accelerometers for motion-tolerant wearable bio-sensors*. in Engineering in Medicine and Biology Society, 2004. IEMBS'04. 26th Annual International Conference of the IEEE. IEEE.
2. Bland, J.M. and D. Altman (1986) Statistical methods for assessing agreement between two methods of clinical measurement. *The lancet*. **327**(8476): p. 307-310.
3. Cazares, S., et al. (2001) Tracking poles with an autoregressive model: a confidence index for the analysis of the intrapartum cardiotocogram. *Medical engineering & physics*. **23**(9): p. 603-614.
4. Chamberlain, J.M., et al. (1998) Pediatric risk of admission (PRISA): a measure of severity of illness for assessing the risk of hospitalization from the emergency department. *Annals of emergency medicine*. **32**(2): p. 161-169.
5. Chan, K. and Y. Zhang. (2002) *Adaptive reduction of motion artifact from photoplethysmographic recordings using a variable step-size LMS filter*. in Sensors, 2002. Proceedings of IEEE. IEEE.
6. Clifton, D., et al. (2007) Measurement of respiratory rate from the photoplethysmogram in chest clinic patients. *Journal of clinical monitoring and computing*. **21**(1): p. 55-61.
7. Coetzee, F.M. and Z. Elghazzawi (2000) Noise-resistant pulse oximetry using a synthetic reference signal. *Biomedical Engineering, IEEE Transactions on*. **47**(8): p. 1018-1026.
8. Deshmane, A.V. (2009) False arrhythmia alarm suppression using ECG, ABP, and photoplethysmogram. 2009, Massachusetts Institute of Technology.
9. Fleming, S., et al. (2008) *Non-invasive measurement of respiratory rate in children using the photoplethysmogram*. in Engineering in Medicine and Biology Society, 2008. EMBS 2008. 30th Annual International Conference of the IEEE. IEEE.
10. Fleming, S.G. and L. Tarassenko (2007) A comparison of signal processing techniques for the extraction of breathing rate from the photoplethysmogram. *World Academy of Science, Engineering and Technology*.
11. Foo, J.Y.A. and S.J. Wilson (2005) Estimation of breathing interval from the photoplethysmographic signals in children. *Physiological measurement*. **26**(6): p. 1049.

12. Gibbs, P. and H.H. Asada. (2005) *Reducing motion artifact in wearable bio-sensors using MEMS accelerometers for active noise cancellation*. in American Control Conference, 2005. Proceedings of the 2005. IEEE.
13. Gil, E., J. María Vergara, and P. Laguna (2008) Detection of decreases in the amplitude fluctuation of pulse photoplethysmography signal as indication of obstructive sleep apnea syndrome in children. *Biomedical Signal Processing and Control*. **3**(3): p. 267-277.
14. Goldberger, A.L., et al. (2000) Physiobank, physiotoolkit, and physionet components of a new research resource for complex physiologic signals. *Circulation*. **101**(23): p. e215-e220.
15. Goldman, J.M., et al. (2000) Masimo signal extraction pulse oximetry. *Journal of clinical monitoring and computing*. **16**(7): p. 475-483.
16. Hayes, M.J. and P.R. Smith (2001) A new method for pulse oximetry possessing inherent insensitivity to artifact. *Biomedical Engineering, IEEE Transactions on*. **48**(4): p. 452-461.
17. Hjorth, B. (1970) EEG analysis based on time domain properties. *Electroencephalography and clinical neurophysiology*. **29**(3): p. 306-310.
18. Jin, L. and J. Jie. (2009) *Detection of Respiratory Rhythm from Photoplethysmography Signal Using Morphological Operators*. in 3rd International Conference on Bioinformatics and Biomedical Engineering, 2009. ICBBE 2009. . IEEE.
19. Johansson, A. (2003) Neural network for photoplethysmographic respiratory rate monitoring. *Medical and Biological Engineering and Computing*. **41**(3): p. 242-248.
20. Johnston, W. and Y. Mendelson. (2004) *Extracting breathing rate information from a wearable reflectance pulse oximeter sensor*. in Engineering in Medicine and Biology Society, 2004. IEMBS'04. 26th Annual International Conference of the IEEE. IEEE.
21. Kay, S.M. and S.L. Marple Jr (1981) Spectrum analysis—a modern perspective. *Proceedings of the IEEE*. **69**(11): p. 1380-1419.
22. Kim, B.S. and S.K. Yoo (2006) Motion artifact reduction in photoplethysmography using independent component analysis. *Biomedical Engineering, IEEE Transactions on*. **53**(3): p. 566-568.
23. Krieger, B., et al. (1986) Continuous noninvasive monitoring of respiratory rate in critically ill patients. *CHEST Journal*. **90**(5): p. 632-634.
24. Krishnan, R., B. Natarajan, and S. Warren. (2008) *Analysis and detection of motion artifact in photoplethysmographic data using higher order statistics*. in Acoustics, Speech and Signal Processing, 2008. ICASSP 2008. IEEE International Conference on. IEEE.
25. Lee, C. and Y. Zhang. (2003) *Reduction of motion artifacts from photoplethysmographic recordings using a wavelet denoising approach*. in Biomedical Engineering, 2003. IEEE EMBS Asian-Pacific Conference on. IEEE.
26. Lee, J. and K. Chon (2010) Respiratory rate extraction via an autoregressive model using the optimal parameter search criterion. *Annals of biomedical engineering*. **38**(10): p. 3218-3225.
27. Lee, J. and K.H. Chon (2010) An autoregressive model-based particle filtering algorithms for extraction of respiratory rates as high as 90 breaths per minute from pulse oximeter. *Biomedical Engineering, IEEE Transactions on*. **57**(9): p. 2158-2167.
28. Lee, J., et al. (2004) Design of filter to reject motion artifact of pulse oximetry. *Computer Standards & Interfaces*. **26**(3): p. 241-249.
29. Leonard, P., et al. (2004) An algorithm for the detection of individual breaths from the pulse oximeter waveform. *Journal of clinical monitoring and computing*. **18**(5): p. 309-312.
30. Leonard, P.A., et al. (2006) An automated algorithm for determining respiratory rate by photoplethysmogram in children. *Acta Paediatrica*. **95**(9): p. 1124-1128.
31. Li, Q. and G. Clifford (2012) Dynamic time warping and machine learning for signal quality assessment of pulsatile signals. *Physiological measurement*. **33**(9): p. 1491.
32. Lovett, P.B., et al. (2005) The vexatious vital: neither clinical measurements by nurses nor an electronic monitor provides accurate measurements of respiratory rate in triage. *Annals of emergency medicine*. **45**(1): p. 68-76.
33. Madhav, K.V., et al. (2011) *A robust signal processing method for extraction of respiratory activity from artifact corrupted PPG signal*. in Recent Advances in Intelligent Computational Systems (RAICS), 2011 IEEE. IEEE.
34. Margolis, P. and A. Gadomski (1998) Does this infant have pneumonia? *JAMA: the journal of the American Medical Association*. **279**(4): p. 308-313.
35. Marple Jr, S.L. (1987) *Digital spectral analysis with applications*. Englewood Cliffs, NJ, Prentice-Hall, Inc., 1987, 512 p. **1**.
36. Meredith, D., et al. (2012) Photoplethysmographic derivation of respiratory rate: a review of relevant physiology. *Journal of Medical Engineering & Technology*. **36**(1): p. 1-7.
37. Nakajima, K., T. Tamura, and H. Miike (1996) Monitoring of heart and respiratory rates by photoplethysmography using a digital filtering technique. *Medical engineering & physics*. **18**(5): p. 365-372.
38. Neuman, M. and N. Wang. (1990) *Motion artifact in pulse oximetry*. in Engineering in Medicine and Biology Society, 1990., Proceedings of the Twelfth Annual International Conference of the IEEE. IEEE.
39. Nijman, R.G., et al. (2013) Clinical prediction model to aid emergency doctors managing febrile children at risk of serious bacterial infections: diagnostic study. *BMJ: British Medical Journal*. **346**.
40. Oppenheim, A.V., R.W. Schaffer, and J.R. Buck (1999) *Discrete-time signal processing*. Vol. 5. 1999: Prentice hall Upper Saddle River.
41. Pardey, J., S. Roberts, and L. Tarassenko (1996) A review of parametric modelling techniques for EEG analysis. *Medical engineering & physics*. **18**(1): p. 2-11.
42. Pearson, G.A. and C.E. into Maternal (2008) *Why Children Die: A Pilot Study 2006 England;(South West, North East and West Midlands), Wales and Northern Ireland*. 2008: CEMACH.
43. Pollack, M.M., K.M. Patel, and U.E. Ruttimann (1997) The Pediatric Risk of Mortality III—Acute Physiology Score (PRISM III-APS): a method of assessing physiologic instability for pediatric intensive care unit patients. *The Journal of pediatrics*. **131**(4): p. 575-581.
44. Proakis, J.G. (2001) *Digital signal processing: principles algorithms and applications*. 2001: Pearson Education India.
45. Reddy, K.A., B. George, and V.J. Kumar (2009) Use of Fourier series analysis for motion artifact reduction and data compression of photoplethysmographic signals. *Instrumentation and Measurement, IEEE Transactions on*. **58**(5): p. 1706-1711.
46. Reddy, K.A. and V.J. Kumar. (2007) *Motion artifact reduction in photoplethysmographic signals using singular value decomposition*. in Instrumentation and Measurement Technology Conference Proceedings, 2007. IMTC 2007. IEEE. IEEE.
47. Relente, A. and L. Sison. (2002) *Characterization and adaptive filtering of motion artifacts in pulse oximetry using accelerometers*. in Engineering in Medicine and Biology, 2002. 24th Annual Conference and the Annual Fall Meeting of the Biomedical Engineering Society EMBS/BMES Conference, 2002. Proceedings of the Second Joint. IEEE.

48. Rusch, T., R. Sankar, and J. Scharf (1996) Signal processing methods for pulse oximetry. *Computers in biology and medicine*. **26**(2): p. 143-159.
49. Rusconi, F., et al. (1994) Reference values for respiratory rate in the first 3 years of life. *Pediatrics*. **94**(3): p. 350-355.
50. Selvaraj, N., et al. (2008) Assessment of heart rate variability derived from finger-tip photoplethysmography as compared to electrocardiography. *Journal of Medical Engineering & Technology*. **32**(6): p. 479-484.
51. Shah, S.A. (2012) Vital sign monitoring and data fusion for paediatric triage. 2012, University of Oxford.
52. Simoes, E., et al. (1991) Respiratory rate: measurement of variability over time and accuracy at different counting periods. *Archives of disease in childhood*. **66**(10): p. 1199-1203.
53. Sukor, J.A., S. Redmond, and N. Lovell (2011) Signal quality measures for pulse oximetry through waveform morphology analysis. *Physiological measurement*. **32**(3): p. 369.
54. Thompson, M., et al. (2008) Using vital signs to assess children with acute infections: a survey of current practice. *The British Journal of General Practice*. **58**(549): p. 236.
55. Weng, J., Z. Ye, and J. Weng. (2006) *An improved pre-processing approach for photoplethysmographic signal*. in *Engineering in Medicine and Biology Society, 2005. IEEE-EMBS 2005. 27th Annual International Conference of the IEEE*.
56. Wertheim, D., et al. (2013) Monitoring respiration in wheezy preschool children by pulse oximetry plethysmogram analysis. *Medical & biological engineering & computing*. **51**(9): p. 965-970.
57. Zhou, Y., et al. (2006) Extraction of respiratory activity from photoplethysmographic signals based on an independent component analysis technique: preliminary report. *Instrumentation Science and Technology*. **34**(5): p. 537-545.

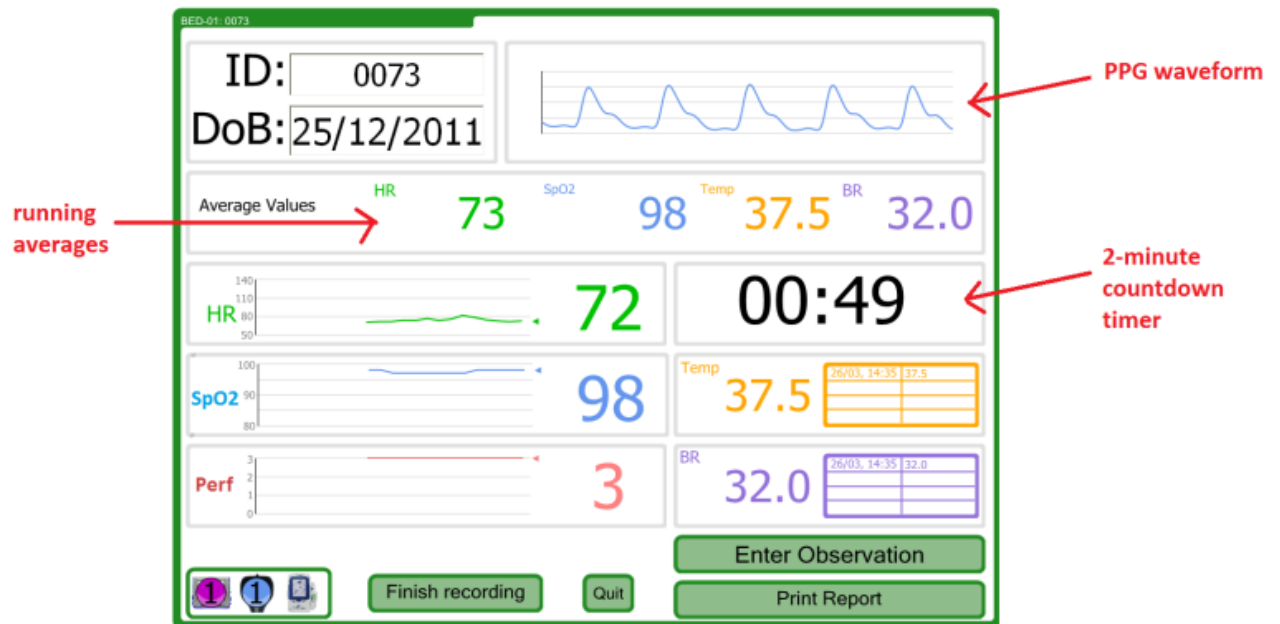


Figure 1: Screenshot of the GUI used in the Pediatric Triage Study. “Perf” gives a measure of peripheral perfusion i.e. the extent of blood supply to peripheral tissues. This measure is automatically provided by the Nonin probe but it was not found to be useful due to the short monitoring period.

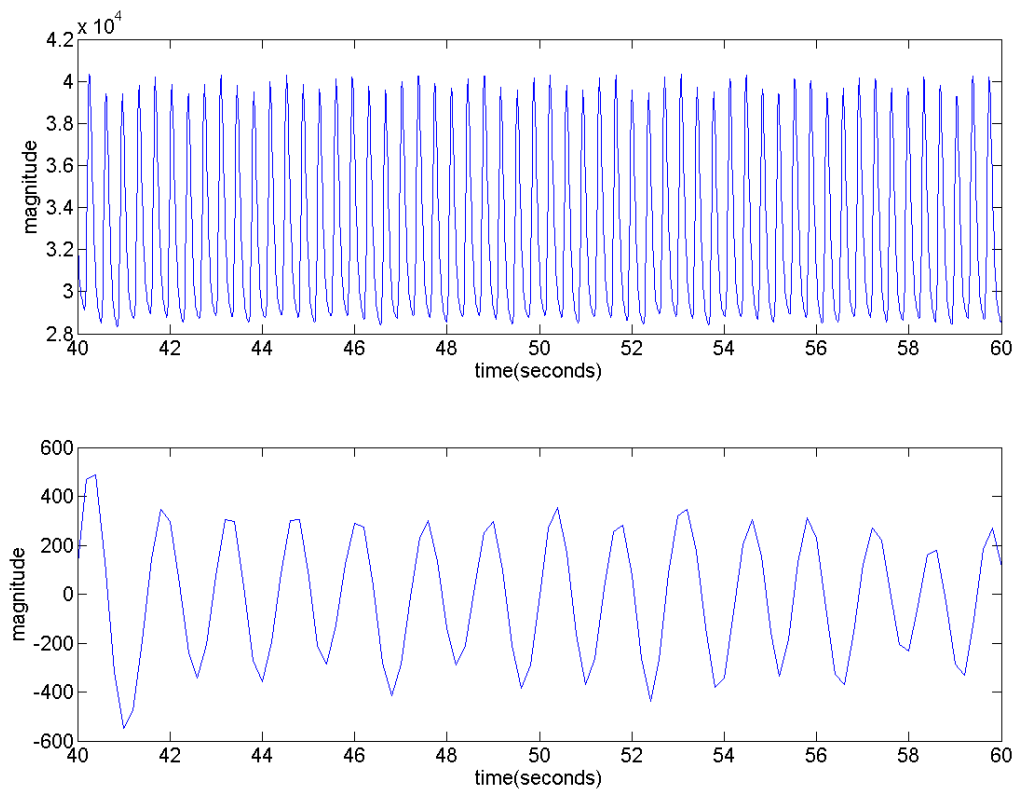


Figure 2: Raw PPG segment (upper plot); output signal after de-trending, low-pass filtering and downsampling to 5 Hz (lower plot).

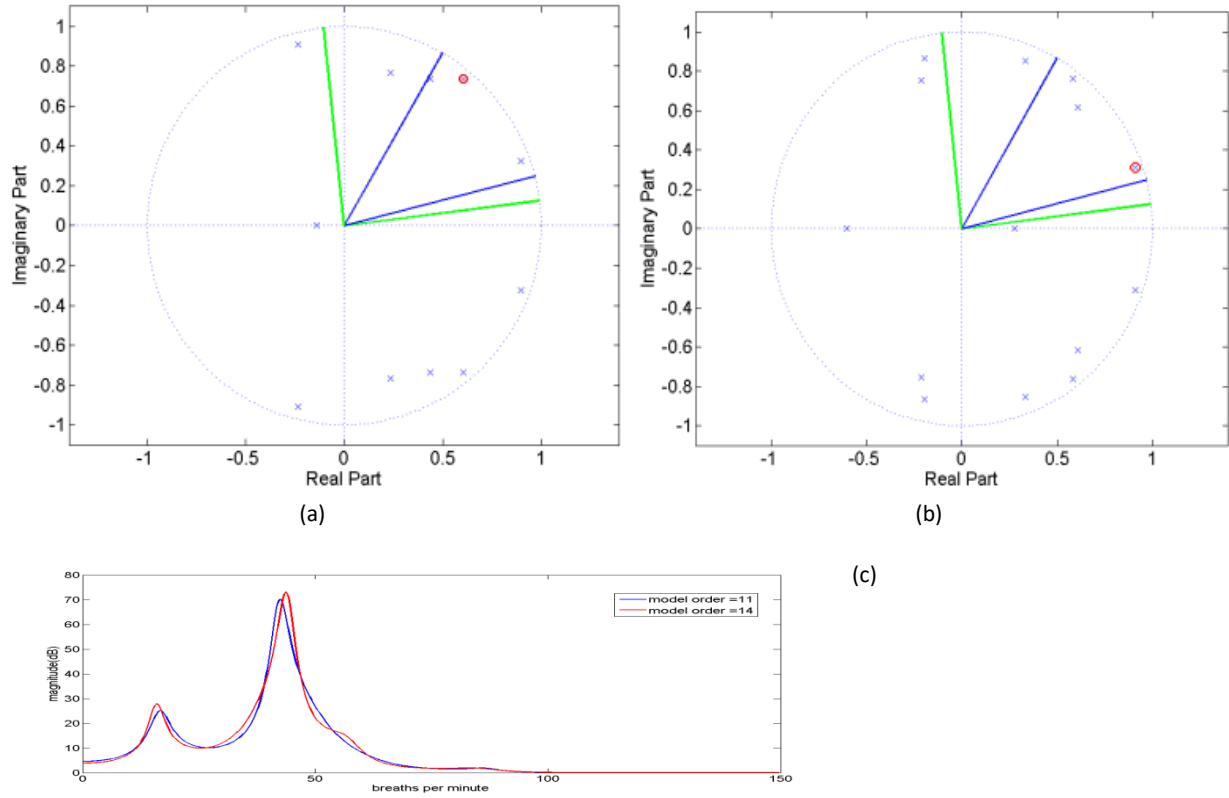


Figure 3: (a) and (b) Pole distribution with the pole with the highest magnitude encircled in red, model order of 11 in (a) and model order of 14 in (b) ; (c) Corresponding frequency spectrum using the poles from the pole-zero plots shown in (a) and (b), 11th order (blue) and 14th order (red) AR models.

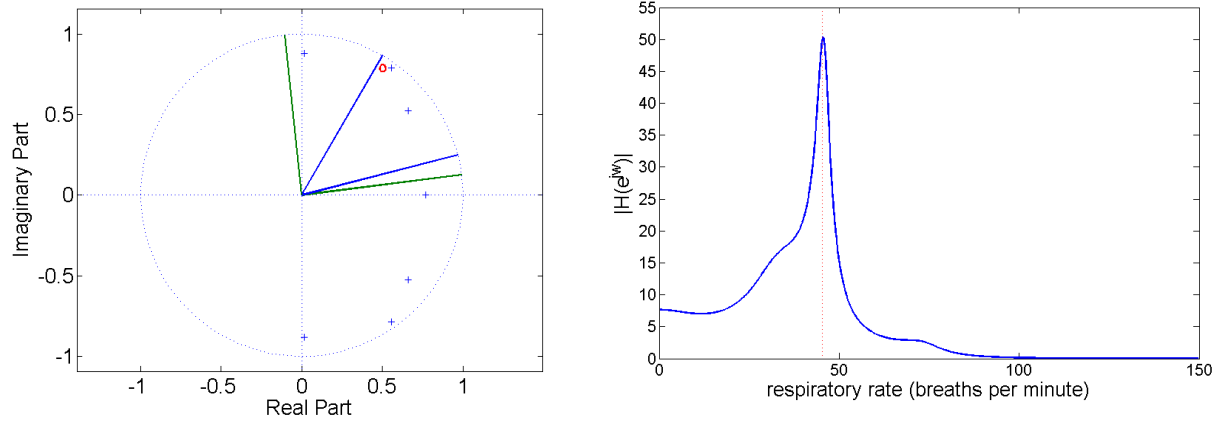


Figure 4: Pole-zero plot with pole with the highest magnitude identified in red for the PPG segment in Figure 2 (left); corresponding frequency spectrum obtained from the poles with peak identified (right).

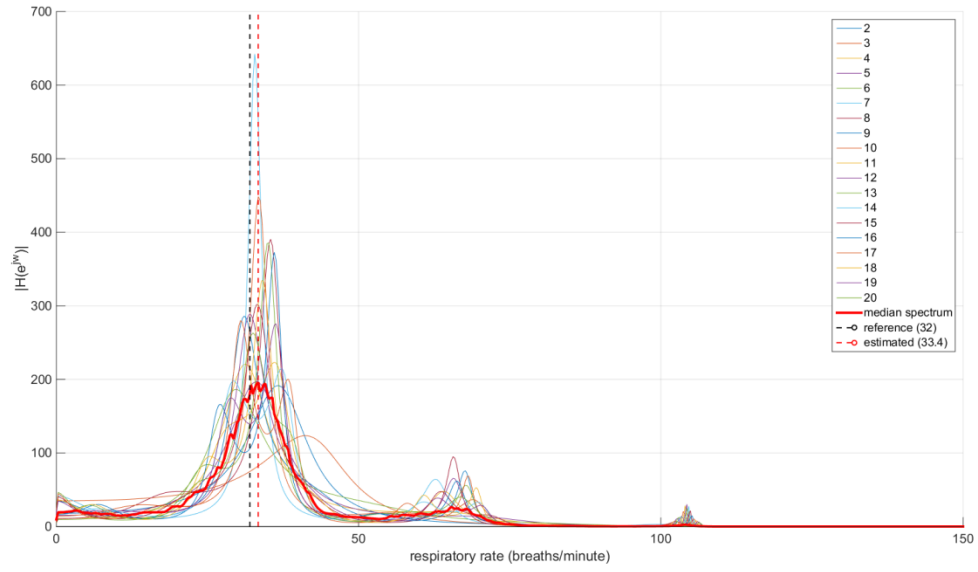


Figure 5: Illustration of median spectrum (red) and the spectrum for model orders 2 to 20, along with the reference (dashed black vertical line) and the estimated respiratory rate (dashed red vertical line) shown.

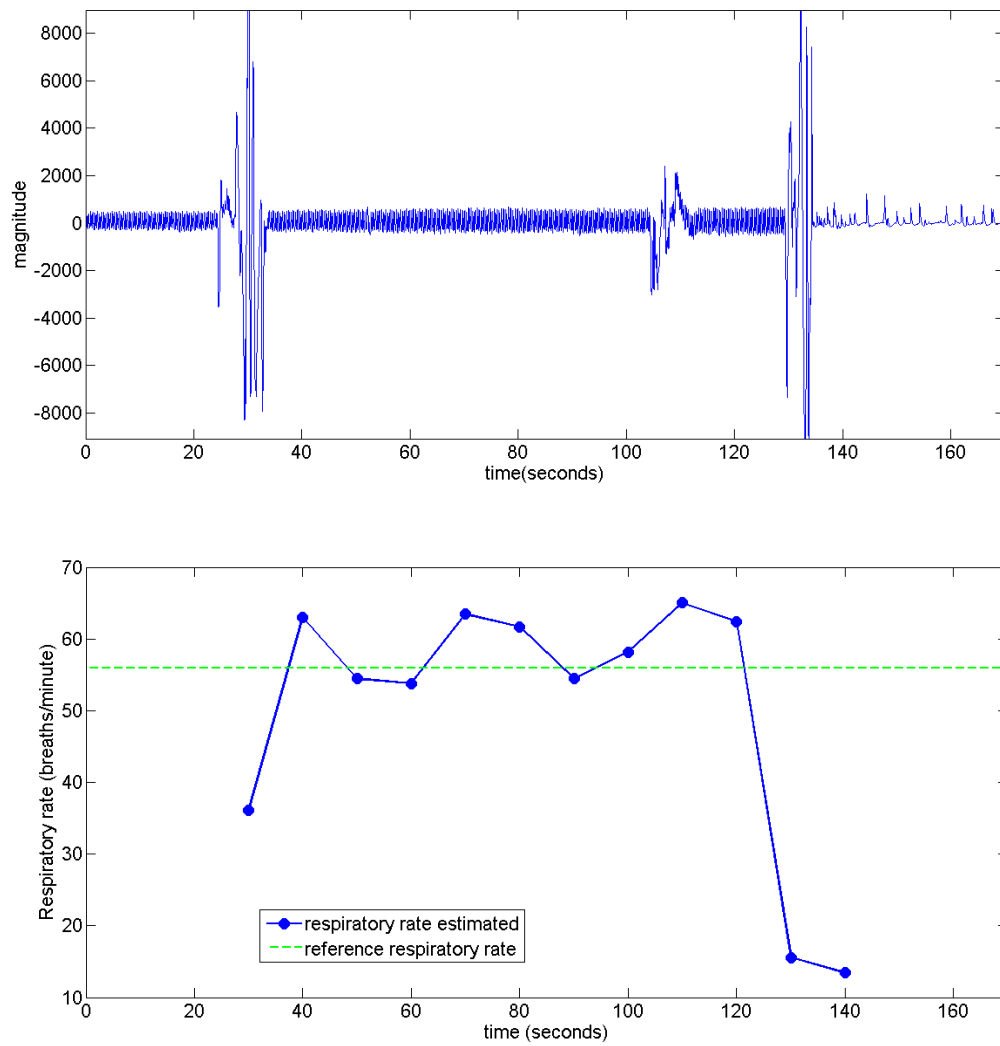


Figure 6: Raw PPG segment from a patient (upper plot); the lower plot shows the respiratory rate estimate, with periods during which the estimation is affected by poor signal quality.

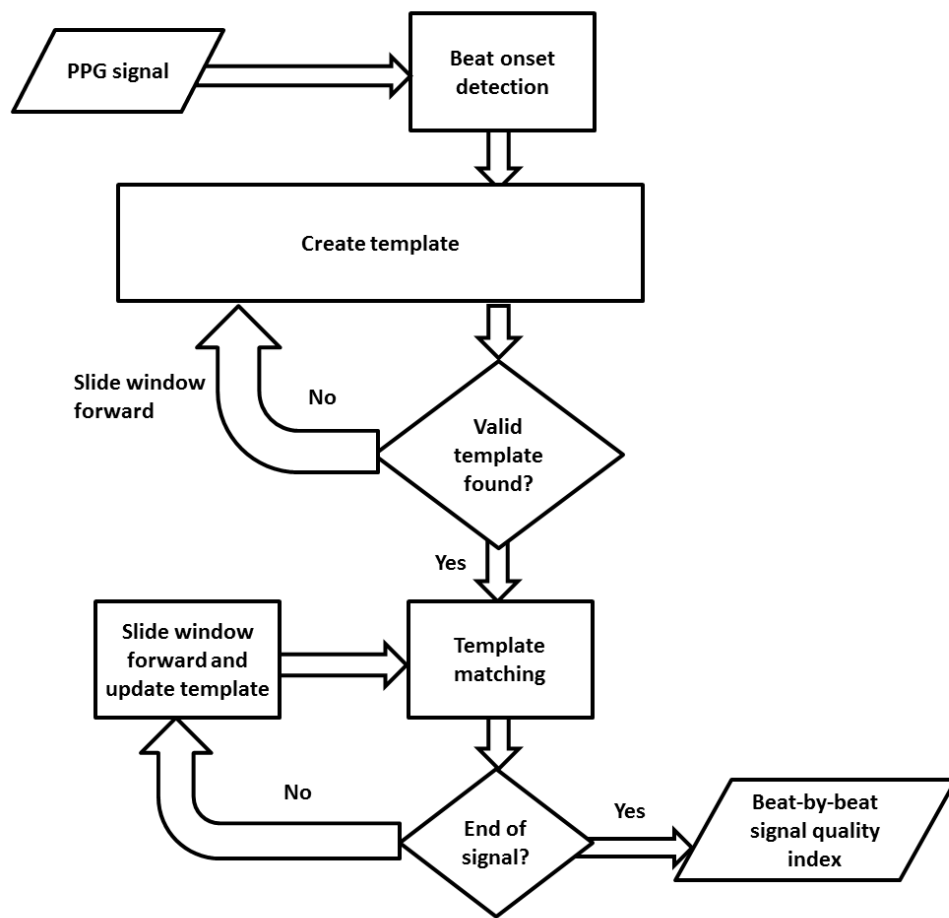


Figure 7: Flowchart of the algorithm for determining Signal Quality Index (SQI)

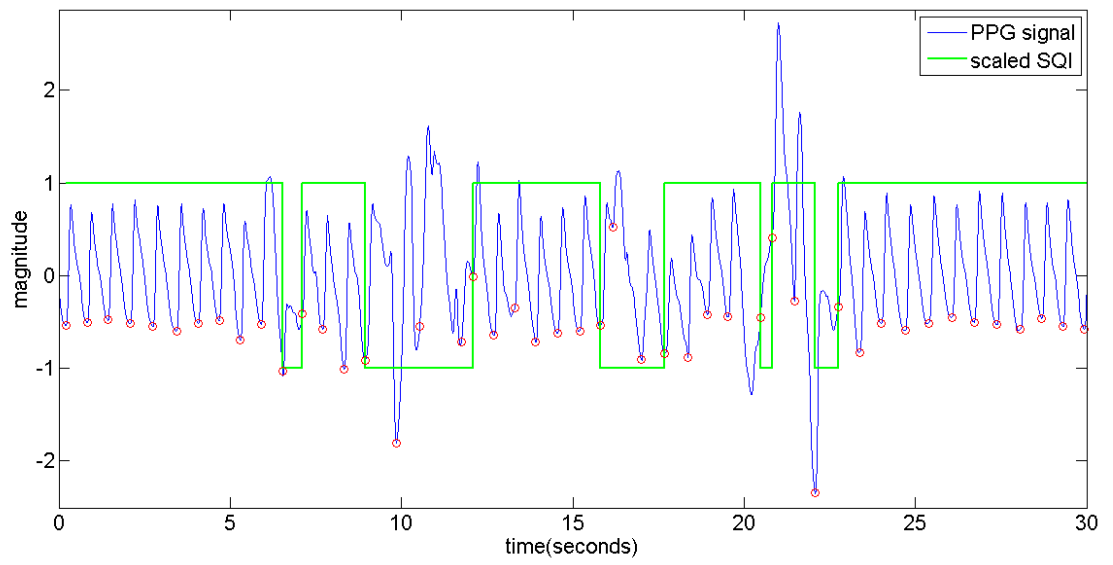


Figure 8: Signal Quality Index (SQI) for a patient shown in green, PPG signal shown in blue and the beat onset instants shown in red

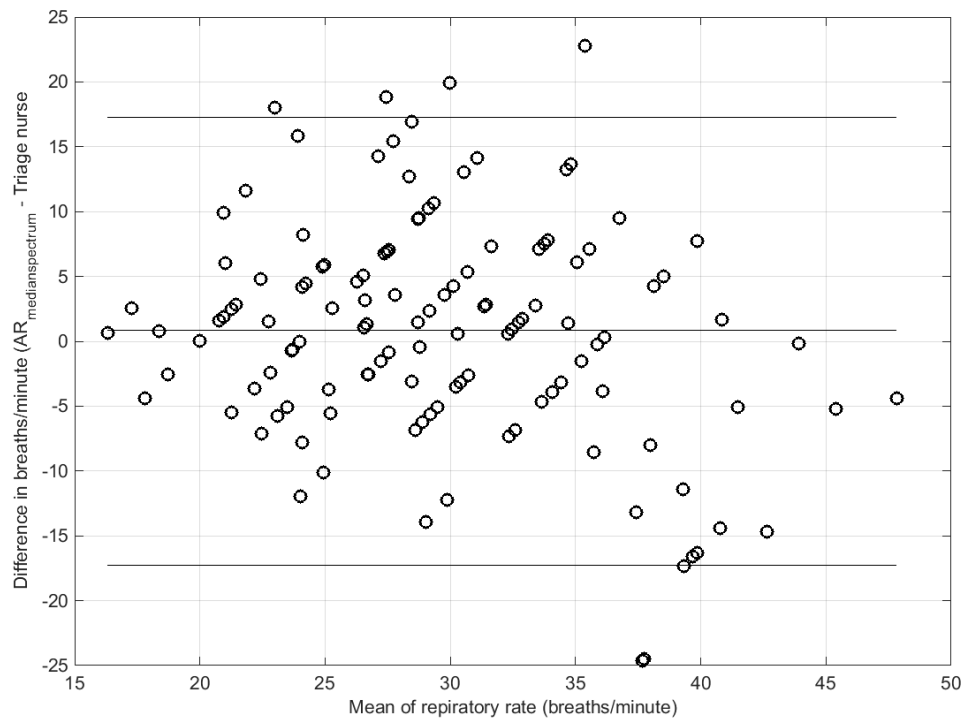


Figure 9: Bland-Altman plot comparing the respiratory rate estimated by the triage nurse and one estimated using *AR_{medianspectrum}* algorithm on 126 patients (with SQI \geq 80%)

Table I
MEAN/MEDIAN ABSOLUTE ERRORS WITH $AR_{original}$, $AR_{spectrum}$ and $AR_{medianspectrum}$ BASED
RESPIRATORY RATE ESTIMATES AND THE REFERENCE RATE (BASED ON ANALYSIS
OF 205 PEDIATRIC PATIENTS)

Method	Mean absolute error (breaths/minute)	Median absolute error (breaths/minute)	Number of patients within 5 breaths per minute of the reference
$AR_{original}$	10.0	7.9	66 (32%)
$AR_{spectrum}$	8.8	5.8	87 (42%)
$AR_{medianspectrum}$	6.7	5.2	103 (50%)

Table II
MEAN ABSOLUTE ERROR OF $AR_{original}$, $AR_{spectrum}$ and $AR_{mediuanspectrum}$ BASED RESPIRATORY
RATE ESTIMATES ACCORDING TO SIGNAL QUALITY

Method	SQ < 80% (n=79)	SQI ≥ 80% (n=126)	SQI ≥ 90% (n=83)
$AR_{original}$	11.3	9.1	8.5
$AR_{spectrum}$	9.2	8.5	7.2
$AR_{medianspectrum}$	7.5	6.2	5.3

Table III
MEAN/MEDIAN ABSOLUTE ERROR OF $AR_{original}$, $AR_{spectrum}$ and $AR_{medianspectrum}$ BASED
RESPIRATORY RATE ESTIMATES IN (0-2y) and (5-12y) AGE GROUPS

Method	Mean Absolute Error		Median Absolute Error	
	0-5 years (n=126)	5-12 years (n=79)	0-5 years (n=126)	5-12 years (n=79)
$AR_{original}$	7.9	13.2	5.9	12.5
$AR_{spectrum}$	7.5	10.8	5.7	7.2
$AR_{medianspectrum}$	7.6	5.3	6.0	4.1